Influence of Shaker Limitations on the Success of MIMO Environment Reconstruction

Marcus Behling
Graduate Research Assistant; Brigham Young University – Department of Mechanical Engineering
mebehlin@student.byu.edu

Matthew S. Allen
Professor; Brigham Young University – Department of Mechanical Engineering
matt.allen@byu.edu

Randall L. Mayes
Mayes Consulting
rajnd75@msn.com

Washington J. DeLima & Jonathan Hower
Honeywell Federal Manufacturing & Technologies
wdelima@kcnsc.doe.gov, jhower@kcnsc.doe.gov

ABSTRACT

Several factors can prevent MIMO environment reconstruction tests from being successful, including the locations of the shakers and their directions, the set of accelerometers that are controlled to, and the upper and lower bounds of a shaker's dynamic range. This work explores these issues for a simple component that flew on a sounding rocket in 2019, and which was instrumented with accelerometers to capture the operational environment in detail. Electrical models were estimated for three modal shakers to predict whether a certain configuration of shakers can recreate the environment without exceeding their input voltage capabilities. Tests are performed controlling to various sets of accelerometers. Finally, the condition number threshold and stinger length are investigated as potential solutions to insufficient shaker dynamic range. These factors are all studied by simulating a MIMO test using transfer functions measured in impact hammer testing, and physical MIMO testing is performed on the most promising test configurations using six modal shakers.

Keywords: Shaker Test, Dynamic Environment, Reconstruction, Dynamic Modeling, Dynamic Range

1. Introduction

To determine if a part can withstand its intended operational environment, vibration qualification tests are performed. In these tests, a shaker is driven to excite the device under test (DUT), hopefully recreating the stresses it experiences in operation. If the part survives the qualification test, it is assumed to be ready to withstand its operational environment. Traditionally, these tests have been performed using a single axis shaker table, wherein the part of interest is rigidly fixed to the table and excited in a single direction. These single axis tests fail to match the DUT's boundary impedance and wrongly excite off-axis motion, often resulting in overly conservative qualification tests; past tests have exceeded the intended environment by 10 to 100 times [1]. Parts sometimes fail these overly conservative tests and must be redesigned when they would have survived in the field environment. This redesign involves more qualification tests which needlessly waste time and money.

One method that has been traditionally used to improve reconstruction accuracy is force limiting. Dynamic environments have historically been created by enveloping an acceleration power spectral density (PSD) with straight lines. This enveloping process along with the impedance mismatch between the operational environment and the shaker table to which the part is mounted in a lab test have historically caused significant over testing at certain frequencies in a bandwidth [1]. If the voltage input to the shaker is notched at these frequencies, the response is reduced. At which frequencies and how much to notch the voltage are decided by force limits. Marchand et al. determined these force limits by multiplying the apparent mass at the shaker-DUT interface by the maximum interface acceleration, finding that this method provided significant notching, particularly at anti-resonances of the Shaker-DUT system [2]. Reyes and Avitabile developed a modular method to minimize shaker-DUT dynamic interactions that have historically caused over testing [3]. Van Fossen and Napolitano proposed a method whereby the forces are computed from a set of acceleration measurements, eliminating the need for load cells, which can be problematic to include the mounting hardware [4].

While force limiting fixes some of the problems associated with single axis testing, off axis motion remains a problem. An alternative to single axis testing is Multiple Input Multiple Output (MIMO) Testing, in which the part of interest is excited in multiple degrees of freedom at the same time. These tests can be performed with six-degree of freedom shaker tables. Paripovic and Mayes showed that these tables could reproduce an acoustic environment in multiple directions much more accurately than a single axis table [5]. While these tables have great potential, they are not yet widely available, and shaker modes can introduce additional uncontrolled dynamics.

Alternatively, MIMO tests can be performed using the Impedance Matched Multi Axis Testing Method proposed in [6], abbreviated as IMMAT. This method involves attaching multiple smaller shakers to the DUT to excite it in multiple directions simultaneously. The shakers are attached via thin metal rods called "stingers" in order to change the DUT's boundary impedance as little as possible in the directions orthogonal to the excitation. While tests performed using the IMMAT Methodology have shown promising results [7], the increased potential for accurate reconstruction comes with increased complexity, which is evidenced by the broad range of relevant studies currently being performed. Rohe et al. performed MIMO tests using various topology optimized fixtures, finding these fixtures to have more modes that are active in a testing bandwidth and to be more difficult to control [8]. Jankowski et al. investigated the effect of the BARC structure's boundary stiffness on its PSD, finding no significant correlation [9]. Schultz and Avitabile presented an algorithm that selects and uses constraint vectors to coordinate input voltage PSDs for multiple shakers [10]. Schultz and Nelson explored how to create a test environment specification in the absence of operational data on a DUT [11]. Pacini et al. showed that a shaker's output force can be distorted due to structural nonlinearities and dynamic interactions between the shaker and structure [12]. Beale et al. compared two methods for selecting accelerometer locations and orientations, finding that both a mean square error minimization and a more complex optimal experimental design method provided reasonable locations [13]. Dumont et al. tested how various accelerometer mounting methods impact measurements, while discussing the potential impact of accelerometer mass on the dynamical properties of a DUT [14]. IMMAT testing requires a target cross spectral density (CPSD) matrix from multiple accelerometers and MIMO control equipment, which is often not available, so traditional vibration testing methods are often employed despite their well-known inaccuracy.

This study is a continuation of [7],[15],[16], and [17]. The DUT is shown in Figure 1; the plate and interface plate together function as a transmission simulator, where forces are applied to the interface plate and transmitted through the plate with the goal of recreating the response on the stool. Tuman et al. found that MIMO tests performed using this configuration yielded more accurate reconstruction results than two other tested configurations where more or less of the flight hardware was included [7]. The plate and stool were each instrumented with three triaxial accelerometers for a total of 18 channels which measured in the radial, spin, and launch directions, and all shakers were attached to the interface plate. The operational environment was obtained from the boost portion of a sounding rocket's flight performed by Kansas City National Security Campus in July 2019. It excludes significant shock events.

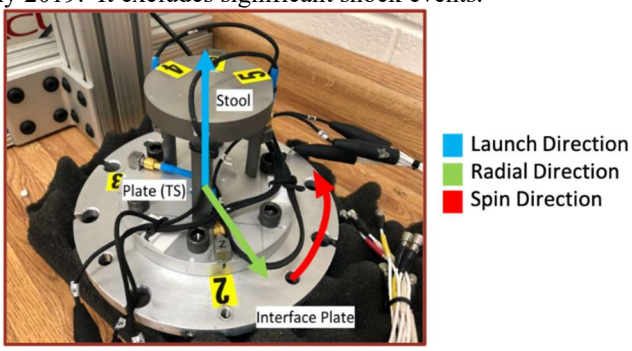

Figure 1*:* DUT Used in MIMO Tests

2. IMMAT Theory

For a linear system, an input F and its steady state response X are related by a frequency response function (FRF) as shown in Eq. (1). For a system with multiple inputs and multiple outputs, the inputs at locations i and outputs at locations s are related by an FRF matrix H, with the superscript "S+TS+V" referring to the system that is being considered, which in this case is the stool (S), transmission simulator (TS), and vehicle (V), which are all present when the DUT's response is measured in the operational environment. The forcing inputs that cause the stool's response in its operational environment can theoretically be determined by inverting the FRF matrix as seen in Eq. (2). Since there are typically more measured outputs than inputs, the inverse of the FRF matrix is generally performed as a Moore-Penrose pseudoinverse, denoted as a "+" in the exponent. Though the distributed drag and thrust loads cannot be recreated in a lab, one could determine the forcing input at many locations on the rocket, attach shakers to each of these locations, and reproduce the operational environment on the stool.

$$X_{s,env}(\omega) = H_{s,i}^{S+TS+V}(\omega) F_{i,env}(\omega) \tag{1}$$

$$F_{i,env}(\omega) = \left(H_{s,i}^{S+TS+V}(\omega)\right)^{+} X_{s,env}(\omega) \tag{2}$$

In a lab, testing the whole rocket is generally not practical, so lab vibration tests use only a part of the vehicle in a lab reconstruction test, reducing the required number of shakers but also changing the DUT's dynamics. The forcing inputs can be determined using Eqs. (3) and (4), where the superscript "S+TS+Sh" refers to the fact that the lab setup includes the dynamics of the stool (S), transmission simulator (TS), and the attached shakers (Sh) which are used to excite the structure.

$$X_{s,lab}(\omega) = H_{s,i}^{S+TS+S}\ (\omega) F_{i,lab}(\omega) \tag{3}$$

$$F_{i,lab}(\omega) = \left(H_{s,i}^{S+TS+Sh}(\omega)\right)^{+} X_{s,lab}(\omega) \tag{4}$$

The goal of a lab vibration test, as previously mentioned, is to recreate the stress state a part will experience in its operation environment. Though strain measurements at various locations on the DUT would be best, it is often assumed that a stress state is accurately recreated if the acceleration response at multiple points on a structure is matched, or if $X_{s,lab} = X_{s,env}$.

In [7], the authors describe two main sources of error in reconstruction tests: error due to modes that shakers cannot control, and errors in the controlled response caused by other factors. Poorly chosen shaker locations, insufficient shaker dynamic range, and poor conditioning in the FRF matrix, among many others, cause this second type of error. This paper discusses possible solutions for some of these sources of error.

3. Simulating a MIMO Test

To predict how successful an IMMAT test will be and to select shaker locations, it is useful to simulate the test beforehand. To perform this simulation, the FRF from input force to the response of each accelerometer channel is necessary. This can be obtained using a finite element model or by performing a roving hammer test at a set of marked locations on the DUT, which is the method employed here. In practice, the target response is calculated as a CPSD matrix to mitigate the effect of noise. The environment CPSD, S_{XX}, can therefore be written as a function of the FRF matrix and some environmental forcing power spectrum, S_{FF}, as shown in Eq. (5). By inverting the FRF matrix, the forcing CPSD of the shakers can be estimated using Eq. (6). This forcing power spectrum can then be inserted into Eq. (5), allowing for estimation of the reconstructed lab response using Eq. (7). We presume that the same control method is employed by the data acquisition system in the MIMO tests presented in this study, except that DAQ obtains the FRF matrix by sending random, uncorrelated voltage inputs to each shaker during a pretest and measuring the responses at each location.

$$S_{XX}(\omega) = H_{XF}(\omega) S_{FF}(\omega) H_{XF}^{*}(\omega) \tag{5}$$

$$S_{FF,EST}(\omega) = {H_{XF}}^{+}(\omega) S_{XX}(\omega) [H_{XF}^{+}(\omega)]^{*} \tag{6}$$

$$S_{XX,EST}(\omega) = H_{XF}(\omega) S_{FF,EST}(\omega) H_{XF}^{*}(\omega) \tag{7}$$

In order to measure the accuracy of the reconstructed response, the error metric used in [7] is employed again here. The PSDs (diagonal terms of the CPSD) of the lab and environment response are converted to decibels, and the root mean square error between the lab and environment for all accelerometer channels is taken at a frequency line as shown in Eq. (8). The Root Mean Square (RMS) of each of these frequency line errors is then taken, resulting in a single error for a given set of accelerometers in Eq. (9). This value is presented for the accelerometers on the plate and the stool in the results that follow.

$$e_{ASD}(f_i) = \sqrt{\frac{1}{n_{accels}} \sum_{k=1}^{n_{accels}} \left[dB[\boldsymbol{S}_{X_k X_k}(f_i)] - dB[\boldsymbol{S}_{X_k X_k,lab}(f_i)]\right]^2} \tag{8}$$

$$e_{ASD} = \sqrt{\frac{1}{n_{freq}} \sum_{i=1}^{n_{freq}} e_{ASD}(f_i)^2} \tag{9}$$

The MIMO simulation can be used to select shaker locations for a MIMO test. Though the simulation would ideally check every potential set of shaker locations, an iterative shaker selection algorithm has been found to yield reasonable results using far fewer calculations [18]. For each potential shaker location, this algorithm simulates the response $S_{XX,EST}$ and calculates the RMS dB Error. The shaker that yields the lowest error is removed from the pool of potential locations and added to a vector of selected locations. The algorithm then selects the next shaker location, iterating through each available location and adding one at a time to the selected locations vector to calculate $S_{XX,EST}$. The best location is kept in the selected locations vector, and this process is repeated until the desired number of shakers is obtained. We have found that many sets of shaker locations yield similar results, so a reasonable set of locations was obtained by selecting shaker locations to excite the modes of the DUT. This setup is shown in Figure 2 and will be referred to as "Setup 1", providing the bulk of the results in this paper. This intuitive set of shakers utilizes the three Q sources on the bottom of the interface plate to control the rigid body vertical, pitch and yaw degrees of freedom, two radial shakers to control the two lateral rigid body modes, and the torsional shaker to give roll rigid body control. Six shakers were used in all the tests in this study. Three Siemens Q Source Miniature Shakers excited the structure in the launch direction. Two Modal Shop (MS) Shakers and a Ling Dynamic Systems (LDS) Shaker excited the structure in the radial and spin directions.

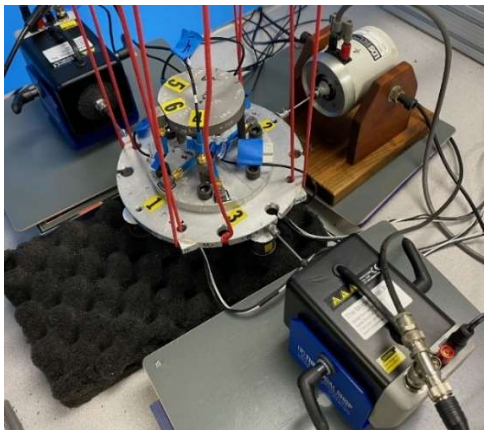

Figure 2*:* MIMO Test Setup 1 (Includes Launch, Spin, and Radial Excitation)

4. Modeling Shaker Dynamics in Simulation

Tests performed using the IMMAT framework tend to use smaller shakers than a traditional shaker table test, so it is possible that shaker voltage limits are exceeded during a test. Hence, it is useful to be able to predict a shaker's RMS voltage in simulation so one can predict whether a certain shaker setup will work. To this end, the dynamic model shown in Figure 3 (similar to the model employed in [12]) was implemented in the MIMO simulation. This model was only implemented for the MS and LDS shakers, as the Q Sources have different dynamics and higher voltage limits than the other shakers. To estimate the values of the model's parameters for each shaker, a uniaxial accelerometer was glued to the head of a 10-32x1/2" bolt which threaded into each shaker's armature (shown in Figure 4), and an experimental FRF from the amplifier voltage to acceleration was obtained. The same FRF was determined analytically from the model, and its magnitude was plotted alongside the magnitude of the experimental FRF. The parameter values were manually varied until the model and experimental FRFs matched with little error. This process was done once for the LDS shaker and once for one of the MS shakers, as it was assumed that both MS shakers would have identical characteristics. While most parameters could be obtained through direct measurement or consultation of the shaker data sheets, some of these parameters were varied from their measured or listed values to match the model FRF to the experimental FRF more closely. The calibration plots and the decided parameter values are shown in the Appendix.

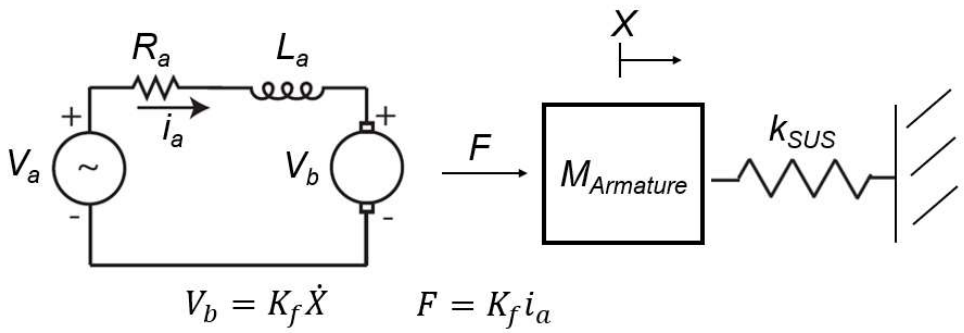

Figure 3: Shaker Model Used to Determine Model Parameters

Figure 4: Setup Used in Shaker Characterization Tests

In order to estimate the FRF between shaker voltage and acceleration for the stool on plate assembly, the FRF obtained from the hammer test was multiplied by the analytical FRF from DAQ voltage to output force, $K_f * i_a$, at each frequency line, resulting in an FRF from voltage to acceleration as shown in Eq. (10). To account for the mass of the DUT and the stiffness of the stinger, this analytical FRF was taken from a slightly different model which is shown in the Appendix. The simulation can then estimate the voltage power spectra for a set of shakers using Eq. (11), and these power spectra can be numerically integrated and square rooted to estimate the RMS voltage as shown in Eq. (12). Note that this is an estimate of the RMS voltage output by the DAQ that is sent to each shaker; this is a more relevant metric than the voltage coming out of the amplifier since most shaker data sheets list voltage limits in terms of the input to the amplifier. The amplifier voltage is obtained by multiplying the DAQ voltage by the amplifier gain.

$$H_{XV}(\omega) = H_{XF}(\omega)H_{FV}(\omega) \tag{10}$$

$$S_{VV,EST}(\omega) = H_{XV}^{+}(\omega)S_{XX}(\omega)[H_{XV}^{+}(\omega)]^{*} \tag{11}$$

$$V_{RMS} = \sqrt{\int S_{VV,EST}(\omega)\, d\omega} \tag{12}$$

Before proceeding, it is important to note that this approach makes one important assumption that could limit the accuracy of these simulations. This approach inherently assumes that the dynamics of the shaker are not affected by its attachment to the structure. In essence, the velocity of the armature of the shaker is assumed to always be the same as it was in the test in Fig. 4. A more accurate approach would be to use substructuring [19] to couple the shaker model to the model of the structure, such that equal displacement (or velocity) is enforced where the shaker joins the structure. Mayes et al. used this approach, finding voltage predictions to be a bit conservative but generally accurate [20]. Unfortunately, this approach requires a drive-point measurement (both force and acceleration) at each point on the structure where the shaker is to be attached, and these are not currently available, so the simple approach outlined above was used instead.

Table 1 compares the RMS drive voltage from a MIMO test using Setup 1 to the RMS voltage predicted in simulation. The simulation predicts RMS voltages that are four to six times larger than those obtained in a test. As seen in Figure 5, the voltage auto spectra from the data acquisition system (which we assume is obtained using Eq. (11)) and the voltage auto spectra predicted in simulation vary noticeably, though the simulation predicts general patterns in the spectra reasonably well. Perhaps these would match more closely if parameters were decided using an optimization algorithm rather than manually; maybe not including the mass of the shaker casing as in [12] causes some of this error. Most likely, the dynamics of the shaker change significantly enough from the configuration in Fig. 4 to the MIMO test configuration that dynamic substructuring is required for a closer match on a spectral basis. The method presented here could still serve as a rough alternative to more rigorous modeling methods if sufficient time and data are not available.

Table 1. Comparison of Simulated RMS Voltage and MIMO Test Drive Voltage

RMS Voltage (V)	Simulation	MIMO Test
MS Shaker 1 (Radial)	.410	.066
LDS Shaker (Radial)	.189	.053
MS Shaker 2 (Spin)	.313	.059

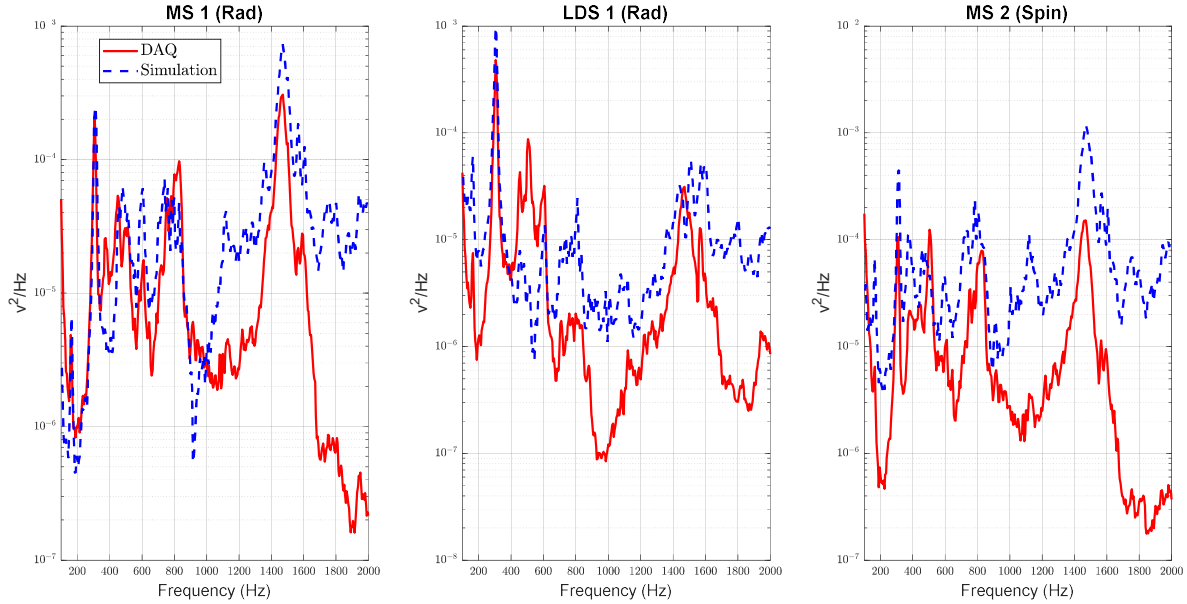

Figure 5. Comparison of DAQ and Simulation Voltage Auto Spectra for Modeled Shakers

5. Effect of Control Accelerometers

References [7], [15], [16], and [17] focused on gaining insight into the transmission of the response from the plate to the stool. As such, they only controlled to the accelerometers on the plate, using the environment data on the stool for comparison only. Since this study is focused less on transmissibility than improving the accuracy of controlled responses, MIMO tests were performed controlling to the plate, stool, and both simultaneously to determine which set of accelerometers yielded the best results. Since these past studies found that the reconstructed plate response was more accurate than the reconstructed stool response when the plate was controlled to, we expected that controlling to the stool would result in decreased stool error and increased plate error. It then seemed logical that controlling to all accelerometers would result in reasonable errors on both components due to the increased challenge of controlling to more accelerometers with a constant number of shakers.

Results of these tests are shown in Table 2, with the "Average Error" being the average RMS dB error over all available accelerometers on the plate and stool. The first two radial channels on the plate were excessively noisy during lab tests, so there were 7 available channels on the plate and 9 available channels on the stool. As expected, the plate error was significantly lower than the stool error when only controlling to the plate. A similar trend was observed for the stool, although the difference between plate and stool error was much less significant in that case. This seems to indicate that there are fewer ways to correctly recreate the stool response than the plate response, which seems reasonable given that the stool is not directly excited in the lab or operational environment while the plate response is. This also underscores how important it can be to choose shaker locations wisely. Controlling to the plate and stool simultaneously yielded the best average results; while this intuitively makes sense, it seemed likely that the increased number of control accelerometers would result in decreased controllability. Though using even more shakers could improve results, the six-shaker setup still yielded the best results on average when controlling to all accelerometers.

While it is difficult to predict how many shakers are generally needed for a given number of control accelerometers, or whether it is best to control to all available data on any given part, controlling to all accelerometers yielded the lowest average error for this DUT, so all tests shown in the remainder of the paper were performed controlling to all accelerometers. It is interesting to note that the simulation tends to result in worse reconstruction than physical tests. This seems reasonable given that the simulation uses FRFs from a Roving Hammer test which approximate the shaker-stinger-DUT FRFs determined and used in a physical MIMO test.

Table 2. Effect of Control Accelerometers on Reconstruction Error

		Control Accelerometers		
		Plate	Stool	Plate + Stool
Simulation	Plate Error (dB)	1.1	8.8	4.8
	Stool Error (dB)	15.7	5.3	8.3
	Average Error (dB)	9.3	6.9	6.8
MIMO Test	Plate Error (dB)	1.4	5.5	4.2
	Stool Error (dB)	11.2	3.5	4.1
	Average Error (dB)	6.9	4.4	4.1

6. Upper Bound of Shaker Dynamic Range

Vibration tests cannot be performed if shaker voltage limits are exceeded in a test. Consider the MIMO test setup shown in Figure 6, which will be referred to as "Setup 2". This setup uses three shakers in the launch direction and three shakers in the radial direction to attempt to control responses in the radial, spin, and launch directions. This setup runs into a couple of problems. First, the shakers "fight" against each other, as one is oriented close to 180 degrees from another. Second, there is no direct torsion input to the DUT. Any spin input to the system is a result of small setup errors that cause eccentricity in the radial shakers. The RMS voltage required of each shaker is artificially increased, and shaker voltage limits are exceeded, preventing a test from running on this setup. Incidentally, a similar setup was chosen in [16] because the modal test data did not contain any DOF in the spin direction, and so the shaker placement algorithm could not select any shakers in the spin direction. In order to address this, it was necessary to glue angle blocks onto the plate and repeat the tests with hammer hits on those blocks.

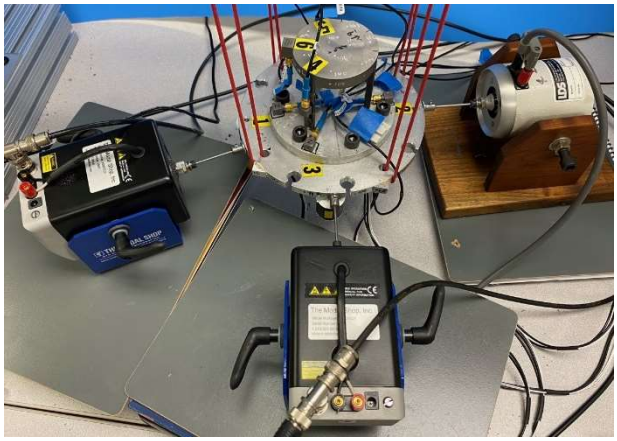

Figure 6. MIMO Test Setup 2 (Includes Launch and Radial Excitation)

One way to lower shaker voltages is to limit them to a specified number of standard deviations around the mean; most controllers have a setting such as this because a random voltage with a Gaussian distribution has the potential to return infinite values, saturating the hardware. In the Data Physics® system used in this study, this is called the Sigma Clip setting. A Sigma Clip of 3 is generally used in vibration tests as three standard deviations includes 99.7% of the data for a gaussian distribution; only the top and bottom .15% of voltages are clipped in such a test. While lowering the Sigma Clip parameter could reduce shaker voltage levels sufficiently to perform a test, it can affect reconstruction results significantly; Kihm and Delaux mention high frequency distortions, reductions in shaker dynamic range, and reductions in damage potential as reasons against reducing the Sigma Clip parameter in vibration fatigue tests [21]. Though fatigue is not being tested here, the same conclusions are likely to apply.

Another option is to implement a condition number threshold on the FRF matrix that is determined in the pretest. Since the FRF matrix is inverted using Eq. (11) to determine the voltage CPSD, frequencies where the FRF matrix is poorly conditioned are particularly sensitive to noise resulting in artificial amplification of the voltage power spectrum at these frequencies. A condition number threshold can be implemented by taking the singular value decomposition of the matrix, calculating the ratio of each singular value to the largest singular value, and truncating the matrix to remove any singular values that are too small, as demonstrated in [7]. The same study found that implementing the condition number threshold tended to cause MIMO test results to match their simulation counterparts more closely; this is generally true, and the effect of the condition number threshold is further investigated here. When we refer to the condition number threshold, we use the

inverse of the condition number as it is traditionally defined. A condition number threshold of .01, for example, removes all singular values that have a condition number of 100 or above, or those singular values that are less than 0.01 times the largest singular value.

Since the condition number threshold is implemented on the FRF matrix, which changes with every set of shaker locations, the effect of the condition number threshold also tends to vary from one set of shaker locations to another; one set of shaker locations can yield a more poorly conditioned FRF matrix than another set. This is demonstrated in Figure 7, which compares the condition number spectrum of the FRF matrix for the two setups shown in Figure 2 and 6. Since Setup 2 controls spin indirectly, the response is very sensitive to a small change in the shaker inputs, and the FRF matrix is poorly conditioned. Implementing a condition number threshold of 0.1 on the FRF matrix allows a test to be performed using Setup 2 because it lowers the required voltage level; the auto spectral densities of the corresponding voltages are shown in Figure 8. Intuitively, the most significant notching in voltage auto spectra occurs at the most poorly conditioned frequency lines. Performing a MIMO test with this setup and a condition number threshold of 0.1 results in the reconstruction shown in Figure 9. As seen in the figure, implementing a large condition number threshold tends to result in undertesting, particularly in valleys in the environment. The condition number threshold is therefore a tradeoff; while it can reduce shaker exertion so that a test can be performed, it removes information from the FRF matrix, resulting in worse reconstruction.

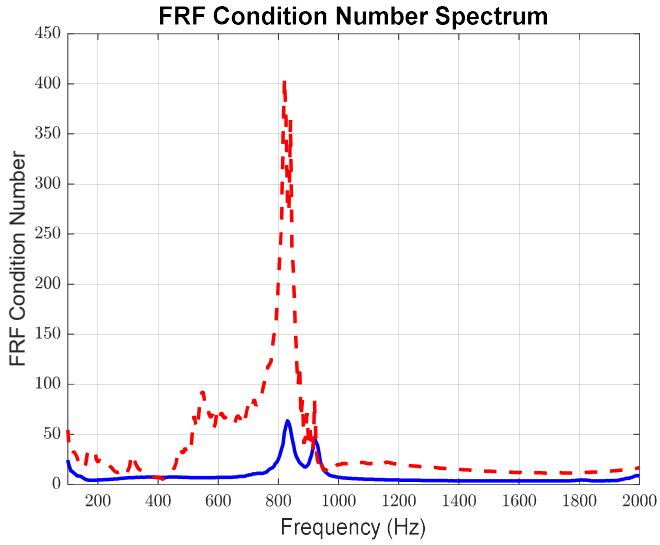

Figure 7. Condition Number Spectrum of MIMO Test FRF for Setup 1 (Blue) and 2 (Red)

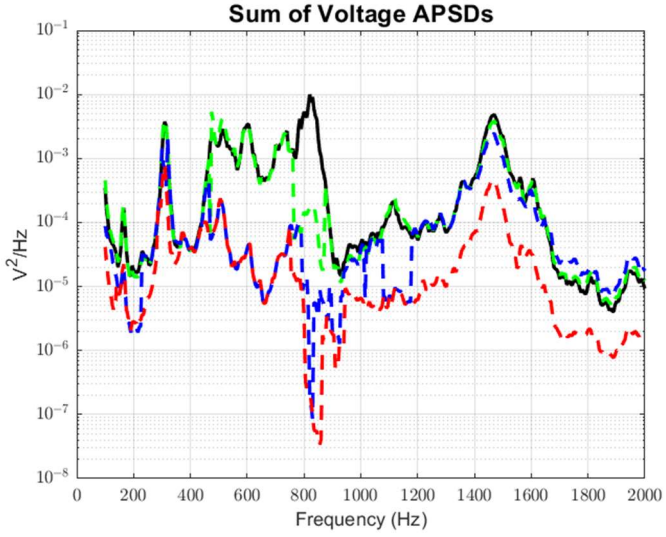

Figure 8. Sum of MIMO Test Voltage Auto Spectra for Setup 2 with a Condition Number Threshold of 0 (Black), 0.01 (Green), 0.05 (Blue), and 0.1 (Red)

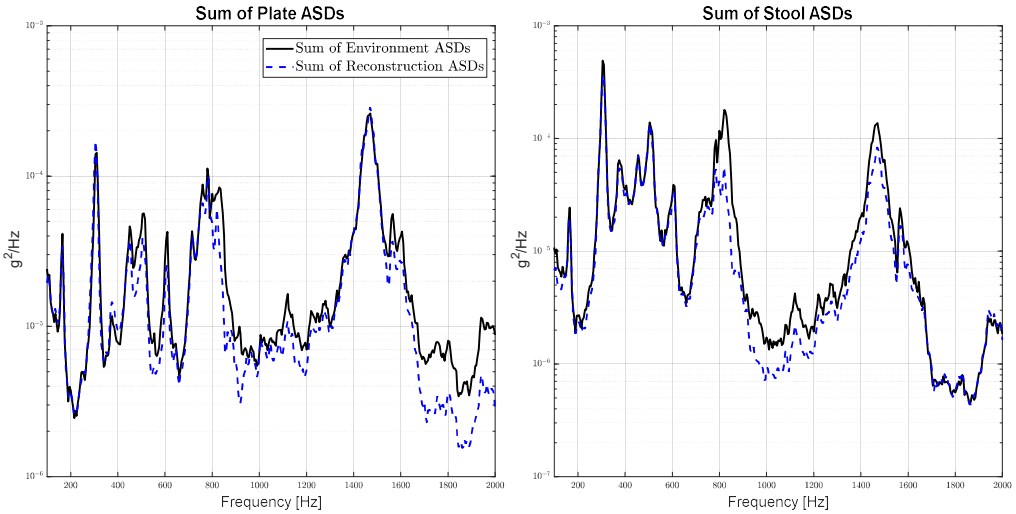

Figure 9. MIMO Test Results for Setup 2 with Condition Number Threshold = 0.1

Now consider Setup 1, shown previously in Fig. 2. Since this setup orients shakers so they fight less and inputs torsion directly, a MIMO test can be performed with no condition number threshold (or the threshold set to zero), reconstructing the environment as shown in Figure 10. Clearly, it is better to avoid implementing a condition number threshold altogether; when a small threshold (~.01) is implemented on this setup, reconstruction results do not change significantly, and when a larger threshold is implemented, results worsen.

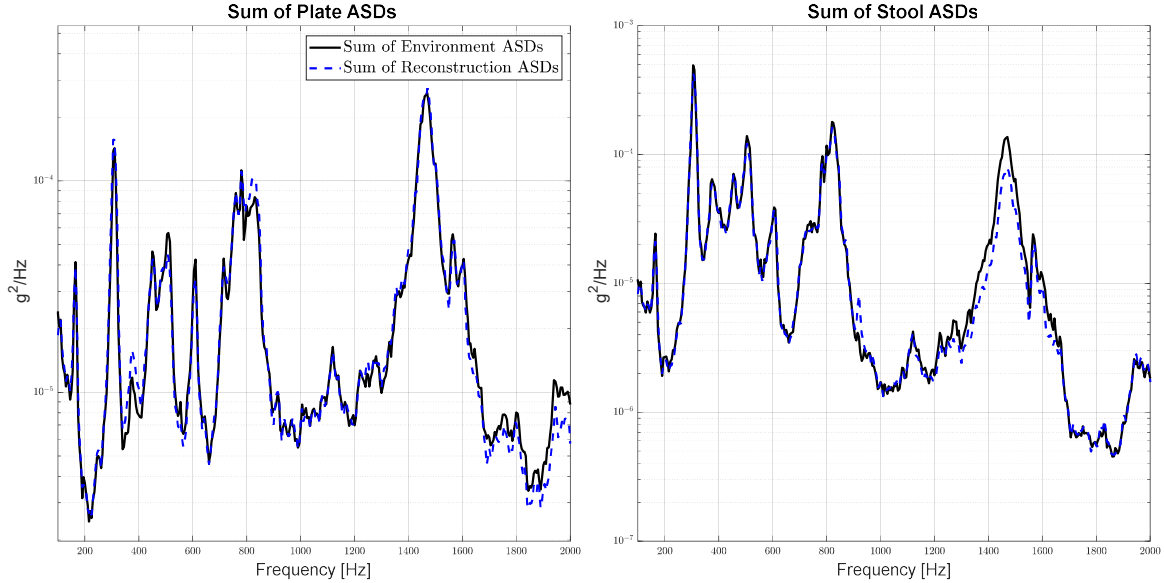

Figure 10. MIMO Test Results for Setup 1 with Condition Number Threshold = 0

A summary of reconstruction results for the two setups is given in Table 3. From these results, we conclude that the condition number threshold is a useful tool that can help tests be performed when shaker voltage limits are exceeded. It should be implemented carefully, though, as it can result in undertesting. It is best to select a set of shaker locations that can run without a condition number threshold or with a very small threshold, such as those in Setup 1, as such a test retains all the information in the FRF matrix, yielding the most accurate reconstruction. A well-conditioned setup seems to be one that minimizes shaker fighting and directly excites the structure in every direction it seeks to control. For a well-conditioned setup, there does not seem to be a good reason to implement a condition number threshold on the FRF matrix. However, for other structures or shakers it may be necessary to implement a threshold even when the shakers are optimally placed.

Table 3. Summary of Reconstruction Results for Setup 1 (includes shaker in the spin direction) and Setup 2 (no shaker in the spin direction)

		Condition Number Threshold	
		0	0.1
Setup 1	Plate Error (dB)	4.2	5.2
	Stool Error (dB)	4.1	6.5
Setup 2	Plate Error (dB)	-	7.5
	Stool Error (dB)	-	9.9

7. Lower Bound of Shaker Dynamic Range

In reference [5], difficulty was encountered in reconstructing an environment at frequencies near a shaker mode as well as a fixed base mode of the DUT; similarly, in [8] it was found that the highest reconstruction error occurred at modes of the fixture-DUT system. A possible explanation for poor control at DUT and shaker armature modes is insufficient shaker dynamic range. Since the DUT response is amplified at a natural frequency, the voltage input must generally be reduced at these frequencies to avoid over testing. If the shaker has insufficient dynamic range, the minimum signal at these frequencies (i.e. due to electrical noise) may be too large to limit the response at the resonance, resulting in over testing.

The shaker armature, stinger, and DUT system can be represented by the dynamic model in Figure 11. The first axial armature natural frequency can be estimated by plotting the FRF from force *F* to the displacement of the DUT *X2*. By modeling the stinger as a spring with stiffness *EA/L*, we can predict what length of stinger is required to move this armature mode out of the testing bandwidth. With an initial stinger length of 0.3 meters, the first axial armature mode was predicted to occur around 1270 Hz. When the stinger was shortened to .05 meters, the first axial armature mode was predicted to occur around 3110 Hz, which is far greater than the upper limit of the testing bandwidth at 2000 Hz. A set of stingers was cut to 0.05 m, and MIMO tests were performed using both sets of stingers in Setup 1.

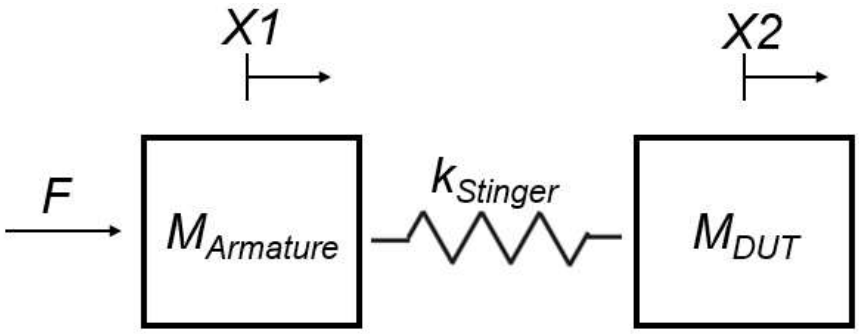

Figure 11. Dynamic Model of Armature-Stinger-DUT System

One way to check if insufficient notching is occurring in a shaker is to compare the predicted and measured voltage auto spectra for a test, where the predicted voltage auto spectra are calculated in the pretest according to Eq. (11). The shakers used in this study were found to have enough dynamic range to control armature modes, so the Sigma Clip parameter was lowered to .8 for the radial and spin shakers to simulate a scenario in which the shaker dynamic range was insufficient. As seen in Figure 12, when longer stingers were used, the shaker could not notch its voltage sufficiently from 1200-1400 Hz, where the armature mode was predicted to occur. When the stinger is shortened, this phenomenon is not observed. As seen in Figure 13, there is significant overshoot from 1200-1400 Hz in the long stinger tests but not in the short stinger tests. Shortening stingers can therefore move a shaker armature mode out of a testing bandwidth, improving control when shakers have insufficient dynamic range.

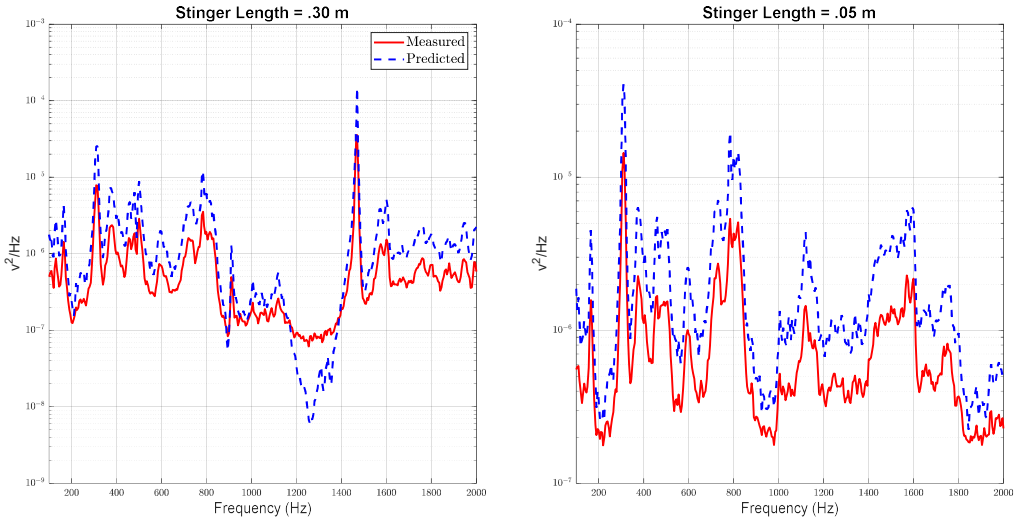

Figure 12. LDS Shaker Predicted and Measured Voltage ASD for MIMO Tests with Long and Short Stingers

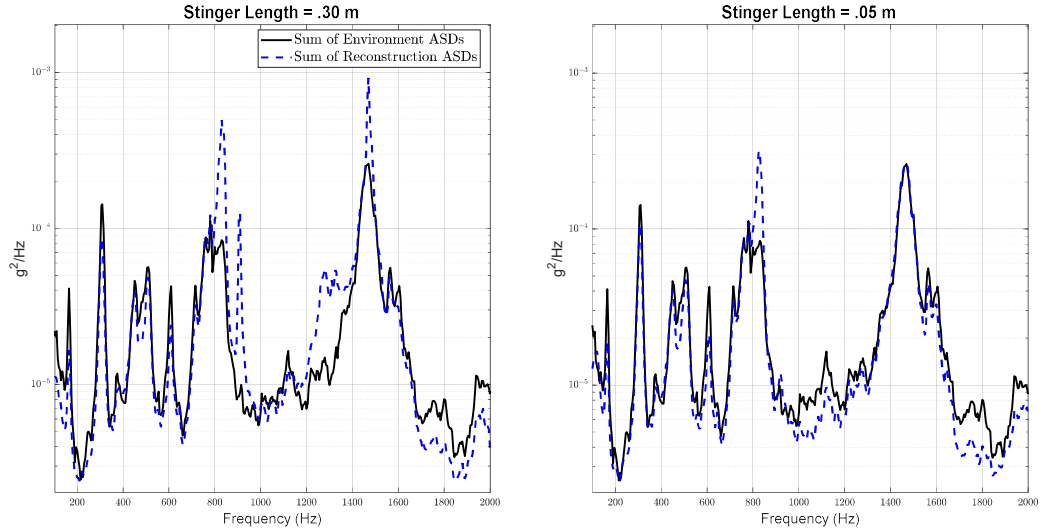

Figure 13. Sum of Plate ASDs for MIMO Tests with Long and Short Stingers

It is worth emphasizing that using shorter stingers only moves the first axial armature mode to a different natural frequency. As seen in Table 4, the reconstruction error increased in the 100-4000 Hz testing bandwidth when using shorter stingers. The control seems to worsen at the armature mode when the shortened stinger is used, so stingers should be shortened if the armature mode cannot be controlled and if shortening the stingers can remove the armature mode from the testing bandwidth.

Table 4. Summary of MIMO Test Results Using Short and Long Stingers (Setup 1)

Stinger Length (m)	0.05		0.3	
Frequency Bandwidth (Hz)	100-2000	100-4000	100-2000	100-4000
Plate Error (dB)	6.1	12.7	7.2	8.5
Stool Error (dB)	6.5	12.9	8.7	10.3

8. Conclusion

This work explored several of the issues that can make environment reconstruction and especially IMMAT testing challenging as compared to traditional single-axis testing. These include selecting shaker locations, selecting control accelerometers, and staying within a shaker's dynamic range. This work demonstrated that a MIMO simulation can be

extremely useful as a tool to predict the performance before performing a physical test, and can be used to help in selecting shaker locations using the iterative selection method introduced in [18]. It also can be used to predict shaker RMS voltages using a simple dynamic model of the shaker-stinger-DUT system. The lowest reconstruction error was found to occur when all available environment data was controlled to. Implementing a condition number threshold on the FRF matrix was found to reduce the required voltage input to each shaker, allowing tests to run that otherwise could not. Using shortened stingers in an IMMAT test was found to raise shaker armature modes, which are uncontrollable without sufficient dynamic range, out of a testing bandwidth, improving reconstruction results. IMMAT testing is certainly complex, but its accuracy can be greatly improved through small changes and simple modeling.

Future work could focus on modifying an environment specification to be more easily matchable in the lab, on modeling shaker dynamics in more detail, or perhaps on increasing the fidelity of the simulation to improve reconstruction in MIMO tests while reducing time wasted. Ultimately, it should focus on developing procedures to optimize the IMMAT testing process so it can be performed quickly on any part and with minimal prior knowledge of the dynamics of the part.

ACKNOWLEDGEMENTS

The authors gratefully acknowledge the Department of Energy's Kansas City National Security Campus, operated by Honeywell Federal Manufacturing & Technologies LLC, for funding this work under contract number DE-NA0002839.

APPENDIX

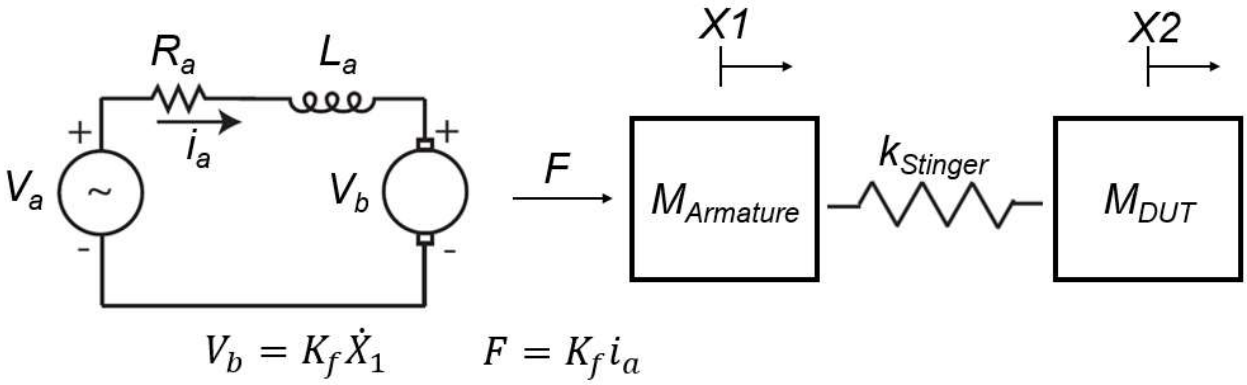

Figure A1. Shaker Dynamic Model Implemented in MIMO Simulation

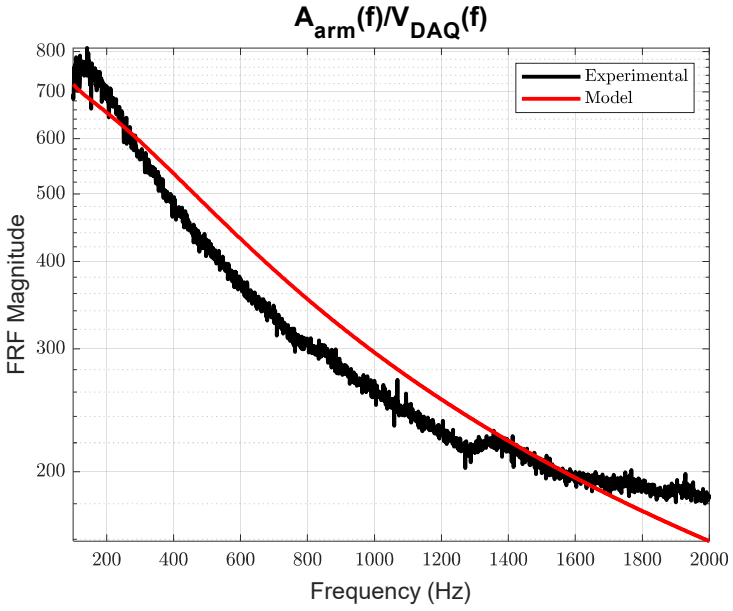

Figure A2. Calibration Plot for MS Shakers

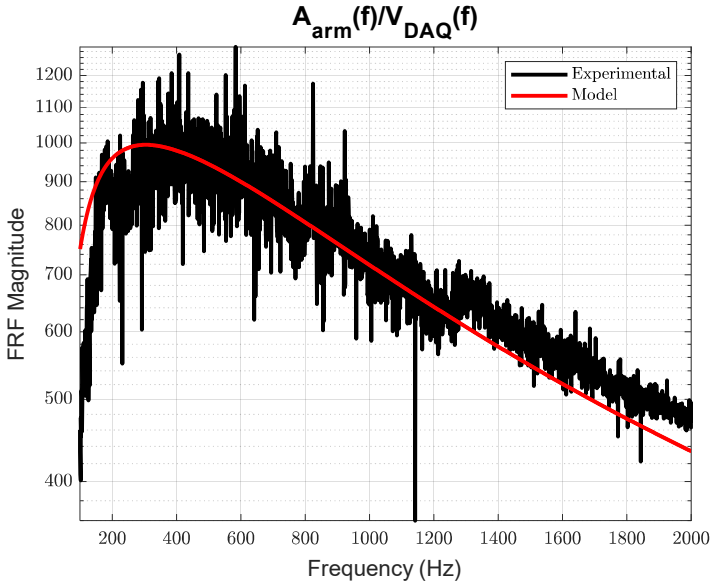

Figure A3. Calibration Plot for LDS Shaker

Table A1. Parameter Values for MS and LDS Shakers

Parameter Name	Value for MS Shakers	Value for LDS Shaker
Resistance (Ω)	.4	1.5
Armature Mass (kg)	.09	.10
Inductance (mH)	.13	.25
Back Emf Constant (V/m/s)	2.4	10
Armature Stiffness (N/m)	2630	2630

REFERENCES

[1] National Aeronautics and Space Administration, "Force Limited Vibration Testing," NASA-HDBK-7004B, 2003. [Online]. Available: http://standards.nasa.gov

[2] P. Marchand, R. Singhal, and M. O'Grady, "Force Limited Vibration Using the Apparent Mass Method," in *Shock & Vibration, Aircraft/Aerospace, Energy Harvesting, Acoustics & Optics, Volume 9*, Cham, 2016, pp. 53–66. doi: 10.1007/978-3-319-30087-0_6.

[3] J. M. Reyes and P. Avitabile, "Force Customization to Neutralize Fixture-Test Article Dynamic Interaction," presented at the International Modal Analysis Conference 36, Orlando, FL, 2018.

[4] T. Van Fossen and K. Napolitano, "An Acceleration-Based Approach to Force Limiting a Random Vibration Test," in *Special Topics in Structural Dynamics & Experimental Techniques, Volume 5*, Cham, 2021, pp. 315–325.

[5] J. Paripovic and R. L. Mayes, "Reproducing a Component Field Environment on a Six Degree-of-Freedom Shaker," in *Dynamic Substructures, Volume 4*, A. Linderholt, M. Allen, and W. D'Ambrogio, Eds. Cham: Springer International Publishing, 2021, pp. 73–78. doi: 10.1007/978-3-030-47630-4_6.

[6] P. M. Daborn, C. Roberts, D. J. Ewins, and P. R. Ind, "Next-generation random vibration tests," 2014, vol. 8, pp. 397–410. doi: 10.1007/978-3-319-04774-4_37.

[7] M. J. Tuman, M. S. Allen, W. J. DeLima, E. Dodgen, and J. Hower, "Balancing Impedance and Controllability in Response Reconstruction," in *Sensors and Instrumentation, Aircraft/Aerospace and Dynamic Environments Testing, Volume 7*, C. Walber, M. Stefanski, and J. Harvie, Eds. Cham: Springer International Publishing, 2023, pp. 133–143. doi: 10.1007/978-3-031-05415-0_12.

[8] D. P. Rohe, R. A. Schultz, T. F. Schoenherr, T. J. Skousen, and R. J. Jones, "Comparison of Multi-Axis Testing of the BARC Structure with Varying Boundary Conditions," in *Sensors and Instrumentation, Aircraft/Aerospace, Energy Harvesting & Dynamic Environments Testing, Volume 7*, Cham, 2020, pp. 179–193.

[9] K. Jankowski, H. Sedillo, A. Takeshita, J. Barba, A. Bouma, and A. Abdelkefi, "Impacts of Test Fixture Connections of the BARC Structure on Its Dynamical Responses," in *Sensors and Instrumentation, Aircraft/Aerospace, Energy Harvesting & Dynamic Environments Testing, Volume 7*, Cham, 2022, pp. 175–177. doi: 10.1007/978-3-030-75988-9_13.

[10] R. Schultz' and P. Avitabile, "Application of an Automatic Constraint Shape Selection Algorithm for Input Estimation," p. 11.
[11] R. Schultz and G. Nelson, "Techniques for Modifying MIMO Random Vibration Specifications," in *Sensors and Instrumentation, Aircraft/Aerospace and Dynamic Environments Testing, Volume 7*, Cham, 2023, pp. 71–83. doi: 10.1007/978-3-031-05415-0_7.
[12] B. R. Pacini, R. J. Kuether, and D. R. Roettgen, "Shaker-structure interaction modeling and analysis for nonlinear force appropriation testing," *Mech. Syst. Signal Process.*, vol. 162, p. 108000, Jan. 2022, doi: 10.1016/j.ymssp.2021.108000.
[13] C. Beale, R. Schultz, C. Smith, and T. Walsh, "Degree of Freedom Selection Approaches for MIMO Vibration Test Design," in *Special Topics in Structural Dynamics & Experimental Techniques, Volume 5*, Cham, 2023, pp. 81–90. doi: 10.1007/978-3-031-05405-1_10.
[14] M. Dumont, A. Cook, and N. Kinsley, "Acceleration Measurement Optimization: Mounting Considerations and Sensor Mass Effect," in *Topics in Modal Analysis & Testing, Volume 10*, Cham, 2016, pp. 61–71. doi: 10.1007/978-3-319-30249-2_4.
[15] M. J. Tuman, C. A. Schumann, M. S. Allen, W. J. Delima, and E. Dodgen, "Investigation of Transmission Simulator-Based Response Reconstruction Accuracy," in *Sensors and Instrumentation, Aircraft/Aerospace, Energy Harvesting & Dynamic Environments Testing, Volume 7*, Cham, 2022, pp. 65–76. doi: 10.1007/978-3-030-75988-9_4.
[16] C. Schumann, M. S. Allen, M. Tuman, W. DeLima, and E. Dodgen, "Transmission Simulator Based MIMO Response Reconstruction," *Exp. Tech.*, May 2021, doi: 10.1007/s40799-021-00454-4.
[17] C. A. Schumann, M. S. Allen, W. J. DeLima, and E. Dodgen, "Transmission Simulator Based MIMO Response Reconstruction for Vehicle Subcomponents," in *Special Topics in Structural Dynamics & Experimental Techniques, Volume 5*, Cham, 2021, pp. 189–195. doi: 10.1007/978-3-030-47709-7_18.
[18] D. P. Rohe, G. D. Nelson, and R. A. Schultz, "Strategies for Shaker Placement for Impedance-Matched Multi-Axis Testing," in *Sensors and Instrumentation, Aircraft/Aerospace, Energy Harvesting & Dynamic Environments Testing, Volume 7*, Cham, 2020, pp. 195–212. doi: 10.1007/978-3-030-12676-6_18.
[19] M. S. Allen, D. Rixen, M. Van Der Seijs, P. Tiso, T. Abrahamsson, and R. L. Mayes, *Substructuring in Engineering Dynamics: Emerging Numerical and Experimental Techniques*. CISM International Centre for Mechanical Sciences: Springer, 2019. [Online]. Available: https://doi.org/10.1007/978-3-030-25532-9
[20] R. Mayes, L. Ankers, P. Daborn, T. Moulder, and P. Ind, "Optimization of Shaker Locations for Multiple Shaker Environmental Testing," *Exp. Tech.*, vol. 44, no. 3, pp. 283–297, Jun. 2020, doi: 10.1007/s40799-019-00347-7.
[21] F. Kihm and D. Delaux, "Vibration Fatigue and Simulation of Damage on Shaker Table Tests: The Influence of Clipping the Random Drive Signal," *Procedia Eng.*, vol. 66, pp. 549–564, Jan. 2013, doi: 10.1016/j.proeng.2013.12.107.